Advances in Materials Research, Vol. 1, No. 3 (2012) 169-182
DOI: http://dx.doi.org/10.12989/amr.2012.1.3.169

The tensile deformation and fracture behavior of a magnesium alloy nanocomposite reinforced with nickel

T.S. Srivatsan*[1], K. Manigandan, C[1]. Godbole[1], M. Paramsothy[2] and M. Gupta[2]

[1]*Division of Materials Science and Engineering, Department of Mechanical Engineering, The University of Akron, Akron, Ohio 443250-3903, USA*
[2]*Department of Mechanical Engineering, National University of Singapore 9, Engineering Drive 1, Singapore 117-576, Singapore*

(Received March 24, 2012, Revised May 26, 2012, Accepted July 12, 2012)

Abstract. In this paper the intrinsic influence of micron-sized nickel particle reinforcements on microstructure, micro-hardness tensile properties and tensile fracture behavior of nano-alumina particle reinforced magnesium alloy AZ31 composite is presented and discussed. The unreinforced magnesium alloy (AZ31) and the reinforced nanocomposite counterpart (AZ31/1.5 vol.% Al_2O_3/1.5 vol.% Ni] were manufactured by solidification processing followed by hot extrusion. The elastic modulus and yield strength of the nickel particle-reinforced magnesium alloy nano-composite was higher than both the unreinforced magnesium alloy and the unreinforced magnesium alloy nanocomposite (AZ31/1.5 vol.% Al_2O_3). The ultimate tensile strength of the nickel particle reinforced composite was noticeably lower than both the unreinforced nano-composite and the monolithic alloy (AZ31). The ductility, quantified by elongation-to-failure, of the reinforced nanocomposite was noticeably higher than both the unreinforced nano-composite and the monolithic alloy. Tensile fracture behavior of this novel material was essentially normal to the far-field stress axis and revealed microscopic features reminiscent of the occurrence of locally ductile failure mechanisms at the fine microscopic level.

Keywords: magnesium alloy; reinforcements; aluminum oxide and nickel particles; metal-matrix composite; microstructure; microhardness; tensile properties; tensile fracture; mechanisms

1. Introduction

The metal magnesium has for long been recognized as a viable engineering alloy for a spectrum of weight-critical applications. In the time period spanning the last three decades, i.e., since the early 1980s, new and improved magnesium alloys that offer a combination of high strength and improved corrosion resistance have been developed and emerged for use in both critical and non-critical end products. Incorporation of hard phases as reinforcements to a magnesium alloy metal matrix does result in improved specific strength (σ/ρ) and specific modulus (E/ρ) when compared one-on-one to the monolithic counterpart (Koss and Copley 1971, Nair 1985, Chawla 1987, Srivatsan and Sudarshan 1993, Ye and Liu 2004). Consequently, composites based on magnesium alloy metal matrices have gradually grown in stature, strength and significance to successfully compete with the

*Corresponding author, Ph.D., E-mail: tsrivatsan@uakron.edu

other monolithic alloys, such as aluminum, steel and titanium, for use in weight-critical applications. The composites have concurrently gained increased attention and acceptance as a potentially viable and economically affordable material for few to several lightweight structural applications. This has been made possible by a synergism of their low density, high specific strength, high damping capacity and other desirable properties (Paramsothy et al. 2011a, Paramsothy *et al.* 2011b). However, from the standpoint of both use in viable applications and end user consideration by way of validation, the magnesium-based composites have received considerably less attention despite revealing noticeable similarity with the aluminum-based composites (Chawla 1987, Srivatsan and Sudarshan 1993). Over the years, sustained research and development efforts have enabled several of the disadvantages associated with magnesium alloys to be overcome by the addition of stiffer and stronger reinforcements to the metal matrix. This has provided the much needed and desired impetus, interest, incentive and inclination towards the use of nano-sized reinforcements to a magnesium alloy metal matrix. Use of nano-scale reinforcements promised a beneficial influence in improved tensile strength, improved compressive strength and even improved ductility when compared one-on-one to the use of micron-size reinforcements (Paramsothy *et al*. 2011a, Paramsothy *et al.* 2011b). Continued research interests and persistent efforts aimed at enhancing the properties offered by nano-scale reinforced magnesium alloy composites resulted in the use of a hybrid reinforcement mixture to complement well with the properties of the two reinforcements used (Paramsothy *et al.* 2011a, Nguyen and Gupta 2008, Habibnejad-Korayem *et al.* 2009, Paramsothy *et al.* 2009). By using a hybrid mixture of reinforcements, it is possible to obtain material properties that cannot be easily obtained by the exclusive use of only one reinforcement to the metal matrix, i.e., magnesium alloy.

Since the early 1980s alloys of magnesium based on the Mg-Al-Zn ternary system have been the focus for few to several research-related studies to keep pace with innovations in the technology sector. Several of these studies have attempted to investigate the use and viability of magnesium-based metal matrix composites (MMCs) for applications in the industries spanning automobile, aerospace and ground transportation systems. Selection and use of both cost effective processing techniques coupled with an appropriate selection of one or more reinforcing phases that has compatibility with the magnesium alloy metal matrix while concurrently enhancing properties of the resultant composite have been the focus of few recent research studies (Paramsothy *et al.* 2009, Gupta and Srivatsan 1999). In few of these studies the researchers have focused their attention towards developing light weight magnesium alloy-based metal matrix composites that offered improved tensile and toughness properties thereby effectively overcoming several of the inadequacies shown by the monolithic, unreinforced counterpart for selection and use in both performance-critical and non-performance-critical applications. As of now there exists no information in the published literature on properties of magnesium alloy-based composites resulting from the addition of nano-sized alumina (Al_2O_3) particles and micron-sized nickel particles as hybrid reinforcement mixture to a magnesium alloy.

In this research paper, an attempt is made to present the results of a study aimed at understanding the influence of dual-phase reinforcements of ceramic (nano-sized alumina particulates (Al_2O_3)) and metal (micron-sized powders of nickel) on microstructural development, hardness, tensile properties and resultant fracture behavior of magnesium alloy AZ31. The fracture surfaces of the samples deformed and failed in uniaxial tension were carefully examined in a scanning electron microscope with the prime objective of examining, understanding and establishing the microscopic mechanism governing quasi-static deformation. Both the monolithic alloy and the dual-phase reinforced composite were prepared by the technique of disintegrated melt deposition (DMD) followed by hot extrusion (Gupta *et al.* 1997, Tham *et al*. 1999, Gupta and Srivatsan 1999, Ling *et al.* 2000, Ganesh *et al*. 2010).

Table 1 Nominal chemical composition of magnesium alloy AZ31

Element	Al	Zn	Mn	Si	Cu	Ca	Fe	Ni	Others	Mg
Max	3.5	1.3	--	0.05	0.05	0.04	0.005	0.10	0.40	Balance
Min	2.5	0.7	0.20							

2. Materials and processing

2.1 Materials

The magnesium alloy used in this research study had a nominal chemical composition, which is summarized in Table 1. This alloy was provided to the National University of Singapore (NUS, Singapore) by Tokyo Magnesium Company Limited (Yokohama, Japan). Blocks of the as-provided AZ31 alloy were carefully sectioned to smaller pieces and then precision machined to remove any and all oxide layers and other visible scales on the surface. All of the surfaces of the magnesium alloy were washed thoroughly with ethanol subsequent to machining. The alumina particles $(Al_2O_3)_p$ having a size of 50 nm along with micron-size nickel particles having a size of 44 microns were used as reinforcements for the AZ31 magnesium alloy to engineer the magnesium alloy-based metal matrix composite. The reinforcing $(Al_2O_3)_p$ particles were procured from Baikowski (Japan) and the reinforcing nickel powder was obtained from Johnson Matthey (USA).

2.2 Processing

2.2.1 Magnesium alloy AZ31

The technique of disintegrated melt deposition (DMD) (Gupta *et al.* 1997, Tham *et al.* 1999, Gupta and Srivatsan 1999, Ling *et al.* 2000, Ganesh *et al.* 2010) was used to cast the monolithic alloy. This process required heating the blocks of AZ31 to 750°C. This heating was accomplished using resistance heating on a graphite crucible and in an inert atmosphere of argon. The graphite crucible had an arrangement for pouring at the bottom. To ensure a near-uniform distribution of the heat, the melt was continuously stirred at 460 rpm for 2.5 minutes. This was made possible using a twin-blade mild steel impeller that had a pitch angle of 45 degrees. To minimize or even avoid interactions between the melt and the mild steel impeller, the impeller was coated with Zirtex 25 (a chemical compound containing 86 pct ZrO_2, 8.8 pct Y_2O_3, 3.6 pct SiO_2, 1.2 pct K_2O and Na_2O with 0.3 pct trace of inorganic). The molten melt was then released through a 10 mm diameter orifice located at the base of the crucible. At a distance of 265 mm from the pouring point the melt was disintegrated using two jets of argon gas (maintained at a flow rate of 25 liters per minute) oriented normal to the melt stream. The disintegrated melt slurry was then deposited onto a metallic substrate located 500 mm from the point of disintegration. The deposition resulted in an ingot whose diameter measured 40 mm.

2.2.2 The nanoparticle composite (AZ31 + 1.5 vol.% Al_2O_3 + 1.5 vol.% Ni)

To form the nanocomposite reinforced with 1.5 vol. pct alumina (Aluminum oxide (Al_2O_3)) and 1.5 pct nickel (44 μm size powder), fine powders of both the reinforcing alumina and nickel were wrapped in aluminum foil having minimum weight (less than 0.5 weight pct) with respect to the magnesium alloy (AZ31). All of the other parameters related to the technique of disintegrated melt

deposition (DMD) were essentially unchanged to that used for the monolithic alloy (AZ31).

Billets of both the monolithic alloy and the dual-phase reinforced composite were precision machined to a size of 36 mm diameter and then hot extruded on a 150 ton hydraulic press using an extrusion ratio of 20.25. The extrusion was carried out at an elevated temperature of 350°C. The billets were held at a temperature of 400°C in a furnace for a period of full 60 minutes prior to extrusion. Colloidal graphite was the lubricant chosen and used during extrusion. The rods obtained following extrusion measured 8 mm in diameter.

3. Experimental procedures

3.1 Sample preparation

The extruded rods of the monolithic AZ31 alloy and alumina particle-reinforced composite (diameter = 8 mm and length = 300 mm) were precision machined to obtain cylindrical specimens that had threaded ends for the uniaxial tension tests. The machining was carried out in conformance with specifications outlined in Standard E-8 of American Society for Testing Materials (ASTM). The major stress axis was taken to be along extrusion direction of the rod stock. The overall length of the specimen measured 2.3 inch (58 mm) with a diameter of 0.25 inch (6.3 mm) at the thread section and diameter of 0.125 inch (3 mm) at the gage section. The gage length measured 0.5 inch (12.5 mm).

3.2 Microstructural characterization

To understand specific influence of processing on (a) grain size and shape and (b) size, shape and distribution of the second-phase particles in the monolithic alloy (AZ31), and the effect of dual particle, i.e., nano-size alumina particulates $(Al_2O_3)_p$ and nickel powder, reinforcements on intrinsic microstructural changes of this composite, initial microstructural characterization of the as-provided extruded rod was carried out. No attempt was made in this study to determine the size of the reinforcing Al_2O_3 particulates dispersed in the magnesium alloy metal matrix. The as-provided extruded rod of AZ31 alloy and the AZ31/1.5 vol.% $(Al_2O_3)_p$/1.5 vol.% Ni composite were prepared for examination in a light optical microscope (Model: Mitutoyo FS70) and photographed using standard bright field illumination technique. Test samples were cut perpendicular to the direction of extrusion and mounted in bakelite. The mounted samples were prepared for optical microscopy observation using standard metallography preparation techniques. Coarse polishing was performed using progressively finer grades (320 grit, 400 grit and 600 grit) of silicon carbide (SiC) impregnated emery paper. Finish polishing to near mirror- like finish was accomplished using 1 micron alumina powder suspended in distilled water as the lubricant. The polished samples were then etched using an etchant. The etchant was acetic-picral, i.e., a solution mixture of 5 ml acetic acid, 6 g picric acid, 10 ml water and 100 ml ethanol. The fine polished surface of the test specimen was then immersed in the etchant till such time a brown film formed and immediately rinsed in running water followed by drying using a hot air gun.

3.3 Mechanical testing

Hardness measurements were performed on polished surfaces of both the monolithic and

composite samples on plane perpendicular to the direction of extrusion. Each reading is the average of four separate measurements taken at random places on the surface of the polished specimens. The test was performed on a Vickers microhardness tester (Model: Tukon 2100) using a load of 200 gram and a dwell time of 15 seconds.

Uniaxial tension tests were performed on a fully-automated, close-loop servohydraulic mechanical test machine (Model: INSTRON: 8500 Plus) in laboratory environment (Relative Humidity of 55 pct) at room temperature (25^{o}C). The servohydraulic machine was equipped with a 22 kip (100 KN) load cell and the tensile tests were performed at a constant strain rate of 0.0001 per second. A PC-based data acquisition software (DAS) was used to record both the stress and strain measurements during the monotonic tension test.

3.4 Failure-damage analysis

A high magnification scanning electron microscope (Model: FEI Quanta 200) was used to examine the fracture surfaces of the deformed and failed tensile samples. Observations were made over a range of magnifications to identify the macroscopic fracture mode and to concurrently establish the key microscopic features on the fracture surface and the mechanisms governing failure. Samples for observation were obtained from the fully deformed and failed tensile test specimens by sectioning parallel to the fracture surface.

4. Results and discussion

4.1 Microstructure

The optical microstructures of the monolithic alloy AZ31 and the dual particle, i.e., nano particle and micron-sized nickel powder, reinforced composite was taken using bright field illumination technique and is shown in Fig. 1. Both the unreinforced alloy and the reinforced magnesium alloy or composite revealed a poly-grained structure but with a noticeable difference in their microstructural features or microstructural intricacies. The dual particle reinforced magnesium alloy composite revealed only a marginal difference in size of the grain (Fig. 1c) when compared one-on-one to the monolithic counterpart (Fig. 1a). The observed marginal difference in grain size of the particulate reinforced magnesium alloy composite is ascribed to be due to the mutually interactive influences of the following competing mechanisms:

(1) A high extrusion temperature of 350^{o}C [T = 0.675 T_M], resulting in conditions conducive for the occurrence of dynamic recrystallization.
(2) The presence of a near uniform dispersion of the two reinforcing phases, i.e., nanosize alumina particles and micron-size nickel powder, which act as potential sites that favor heterogeneous nucleation during solidification. This was made possible by minimizing gravity-related segregation through a proper selection of the stirring parameters for processing of this composite.

The monolithic alloy (AZ31) revealed a duplex microstructure consisting of light colored alpha (α) phase and dark colored eutectic phase (β), which was distributed both at and along the grain boundaries (Fig. 1a). The alumina nanoparticulate and nickel particle reinforced magnesium alloy revealed a heterogeneous distribution of the reinforcing nickel particles through the microstructure

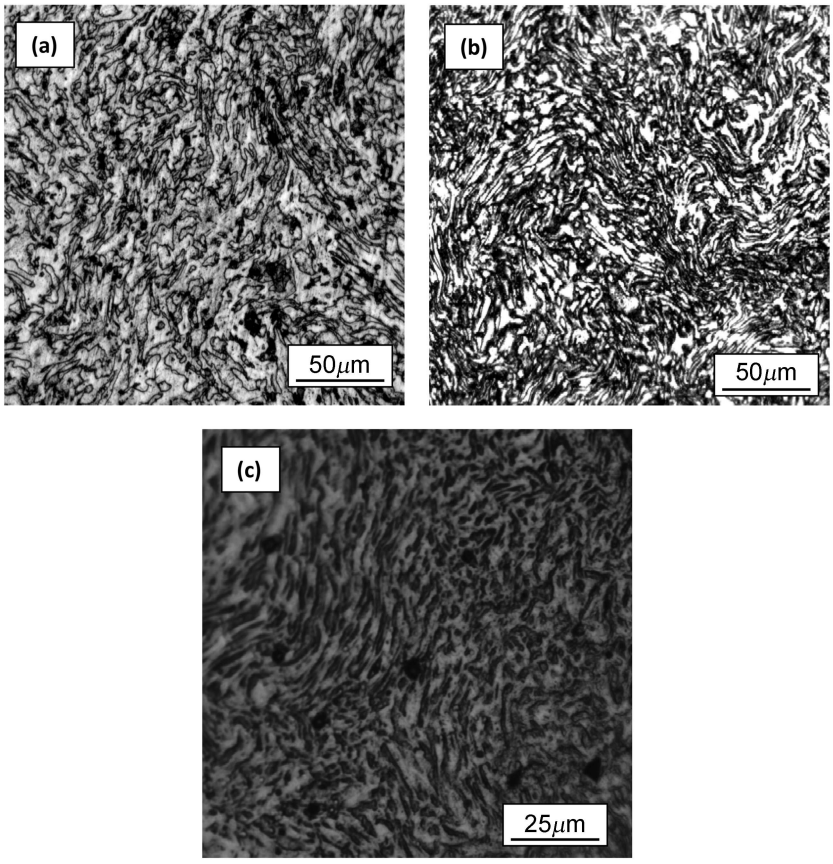

Fig. 1 Optical micrographs showing undeformed microstructure of: (a) Alloy AZ31, (b) AZ31 reinforced with nano Al_2O_3 particles and (c) Alloy AZ31 reinforced with nano Al_2O_3 particulates and micron size nickel powder particles

with regions of particle agglomeration resulting in nickel-particle rich and nickel particle-depleted regions (Fig. 1c). Earlier studies have used the technique of X-ray diffraction and identified the eutectic phase (β) to be the intermetallic particle [$Mg_{17}Al_{12}$] (Paramsothy *et al*. 2011a, Paramsothy *et al*. 2011b). The presence of a higher volume fraction of the eutectic phase (β) was observed in the reinforced magnesium alloy when compared one-on-one with the unreinforced counterpart (Fig. 1a). However, no attempt was made in this study to determine the volume fraction of the β phase in the two materials, i.e., the reinforced magnesium alloy and the unreinforced counterpart.

4.2 Microhardness

The microhardness values are tabulated in Table 2. Results reveal the average hardness of the composite containing two reinforcements, i.e., nanoalumina particulates and micron-size nickel powder particles is 109.5 kg/mm^2, which is 21 pct more than the micro-hardness of alloy AZ31 reinforced with nano-particulates of alumina (Al_2O_3), i.e., 90.25 kg/mm^2 and 72 pct. more than the microhardness of the monolithic alloy AZ31 (i.e., 63.75 kg/mm^2). The observed increase in hardness

Table 2 A listing and comparison of the Vickers microhardness of the three candidate materials

Material		Trials				Vickers hardness	
		Trail 1	Trail 2	Trail 3	Trail 4	Average hardness (Kg/mm^2)	Average hardness (GPa)
AZ31	*D*1 (μm)	75.26	74.57	80.82	71.67	-	-
	*D*1 (μm)	73.32	76.84	84.41	72.81	-	-
	Hv (kg/mm^2)	67	65	54	69	63.75	0.62475
$AZ31+Al_2O_3$	*D*1 (μm)	64.17	64.26	66.56	62.7	-	-
	*D*1 (μm)	64.45	63.89	64.63	62.47	-	-
	Hv (kg/mm^2)	90	90	86	95	90.25	0.88445
$AZ31+Ni+Al_2O_3$	*D*1 (μm)	41.54	40.76	42.6	42.92	-	-
	*D*2 (μm)	40.39	39.61	41.12	40.59	-	-
	Hv (kg/mm^2)	111	115	106	106	109.5	1.0731

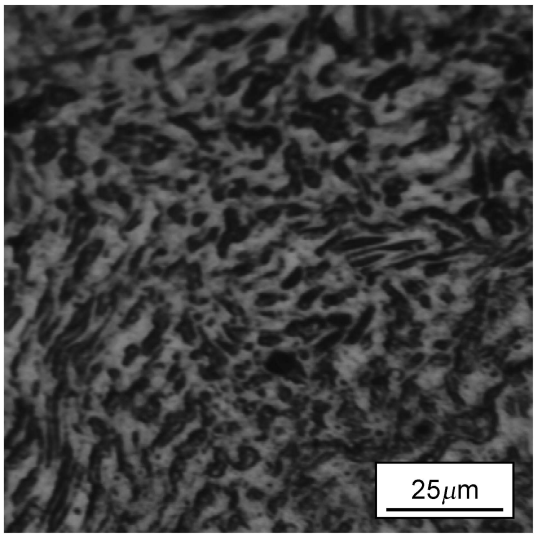

Fig. 2 Optical micrographs showing the key microscopic features to include heterogeneous distribution of the nickel particles in the microstructure of magnesium alloy AZ31 reinforced with nano Al_2O_3 particles

arising from an integration of the reinforcing phases with the magnesium alloy metal matrix has been reported in the published literature for the following:

(1) Magnesium-4.2 pct Zn- rare-earth alloy reinforced with fibers of alumina (Yong and Clegg 1999).
(2) Elemental magnesium reinforced with alumina (Al_2O_3) (Hassan and Gupta 2006, Francis *et al.* 2011).
(3) Magnesium alloy AZ31 reinforced with nano-particulates of alumina (Nguyen and Gupta 2008, Paramsothy *et al.* 2009, Radi *et al.* 2010).
(4) Magnesium alloy AZ91 reinforced with particulates of SiC (Deng *et al.* 2010).

(5) Magnesium alloy AZ91 reinforced with particulates of copper (Ho *et al.* 2004) and
(6) Magnesium alloy AZ92 reinforced with fine particulates of SiC (Seshan *et al.* 2003).

At the "local" level the observed increase in micro-hardness of this dual particle reinforced magnesium alloy metal matrix can be ascribed to the conjoint and mutually interactive influences of the following mechanisms:

(1) Strengthening arising from restricting or impeding the motion of dislocations through the composite microstructure.
(2) Presence and distribution of the reinforcing second-phase particles (nano size Al_2O_3 and micron-size nickel) in the soft magnesium alloy metal matrix achieved by optimum processing.
(3) A refinement in grain size of the magnesium alloy metal matrix arising from the "pinning" effect caused by both the nano-size alumina (Al_2O_3) particulate reinforcements and micron-size nickel powder particles.

4.3 Tensile behavior

The uniaxial tensile properties of this dual particle reinforced magnesium alloy composite along with the nano-alumina particulate reinforced metal matrix composite (AZ31/Al_2O_3) and the monolithic or unreinforced matrix alloy (AZ31) are summarized in Table 3. The values recorded are the mean values based on duplicate tests. An attempt is made to understand the synergistic and mutually interactive influences of the two reinforcing phases in governing the macroscopic mechanical behavior and the fine microscopic mechanisms governing deformation under uniaxial loading. This enables us to make the following observations from the test results.

1. A marginal seven percent increase in the Young's modulus [*E*] of the AZ31/1.5 vol.% Al_2O_3/Ni composite when compared to the monolithic alloy AZ31, and a near similar value when compared to the matrix alloy (AZ31) reinforced with nanoparticles of alumina (Al_2O_3).
2. Only a five percent increase in yield strength of the nickel particle reinforced nanocomposite when compared to the monolithic alloy. However, a noticeable six percent decrease in yield strength of the dual particle reinforced magnesium alloy (AZ31) (σ_y = 215 MPa) when compared with the matrix alloy (AZ31) reinforced with nanoparticulates of alumina (Al_2O_3) (σ_y = 228 MPa).
3. Also, the dual particle reinforced magnesium alloy based composite showed hardly any change in elongation to failure but a 45 pct increase in reduction-in-cross-sectional area (*RA* = 23.7 pct) when compared one-on-one with the monolithic counterpart (AZ31) (*RA* = 16.4 pct).

Table 3 Room temperature tensile properties of the candidate materials (Values are the mean based on duplicate tests)

Specimen	Elastic modulus		Yield strength		UTS		Elongation *GL*=0.5"	Reduction in area	Tensile ductility y $\ln(A_o/A_r)$
	ksi	GPa	ksi	MPa	Ksi	MPa	(%)	(%)	(%)
AZ31	6567.0	45.30	29.55	203.85	42.7	294.0	13.15	16.40	17.95
AZ31+Al_2O_3	7054.5	48.65	33.10	228.35	43.9	303.0	10.85	25.35	29.45
AZ31+Al_2O_3+Ni	6921.1	47.61	31.275	214.94	37.1	256.4	13.64	23.70	23.73

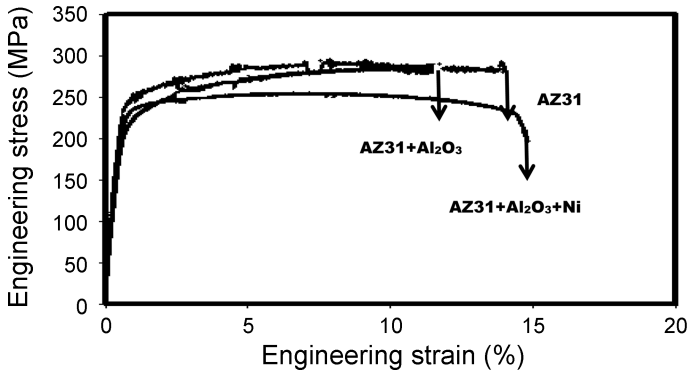

Fig. 3 A comparison of the engineering stress versus engineering strain curves of the unreinforced alloy (AZ31) with the nanoparticle reinforced alloy (AZ31 + Al_2O_3) and the dual particle reinforced magnesium alloy (AZ31 + Al_2O_3 + Ni)

4. The ultimate tensile strength of the nickel particle reinforced magnesium alloy composite was 16 pct lower than the metal matrix reinforced with nano alumina particulates and 15 pct lower than the monolithic unreinforced (AZ31) counterpart.

The engineering stress versus engineering strain curve for the composite is compared with both the matrix alloy reinforced with nanoparticulates of alumina (AZ31/1.5 vol.% Al_2O_3) and the unreinforced matrix alloy in Fig. 3. This figure reveals the dual particle reinforced composite to have marginally lower yield strength and noticeably lower tensile strength than both the monolithic alloy (AZ31) and the monolithic alloy reinforced with nanoparticulates of alumina (Al_2O_3). However, the ductility, quantified by strain-to-failure, is noticeably larger for the dual particle reinforced magnesium alloy metal matrix (AZ31) composites than the monolithic (AZ31) counterpart. Based on microstructure the yield strength of this dual particle reinforced magnesium alloy composite can be predicted using the relationship (Mao 2010, Dieter 2007)

$$\sigma_y = \sigma_O + \sigma_S + \sigma_g + \sigma_{s-p} + \sigma_d$$

Where in this expression σ_O is the lattice friction stress and σ_S and σ_g are strengthening contributions from the solid solution and grain size. Also σ_{s-p} is the contribution from second-phase particles dispersed through the alloy microstructure and σ_d is contribution to strength from dislocation density. Based on experimental values obtained for both the reinforced and unreinforced magnesium alloy it is clear that contributions to strength from grain size refinement, second-phase particle presence and distribution and dislocations is only marginal to the strengthening provided by the solid solution, as for the monolithic alloy (AZ31). Contributions, if any, by way of precipitation hardening provided by both the nanometer size Al_2O_3 (alumina) particulates and the fine micron size nickel particles present in the composite microstructure is ignored since it is bound to be a very small contribution to the overall strength of the composite material.

4.4 Tensile fracture behavior

In this section the tensile fracture behavior of the dual particle reinforced magnesium alloy

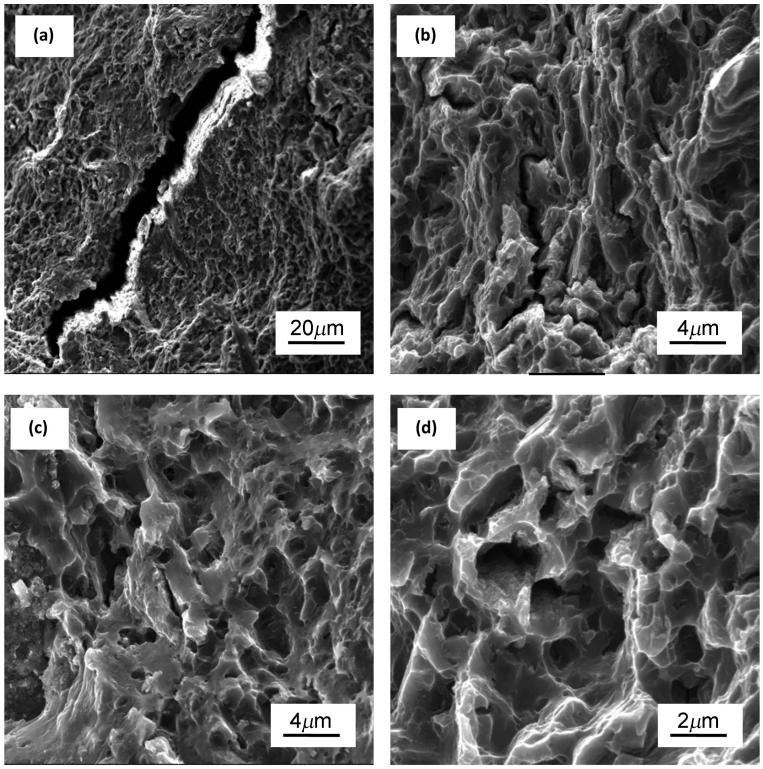

Fig. 4 Scanning electron micrographs of the tensile fracture surface of the AZ31 + Al_2O_3 + Ni composite showing: (a) Overall morphology macroscopically brittle with macro-cracking, (b) Transgranular region covered with a noticeable population of ductile dimples, (c) Region prior to tensile overload covered with microscopic voids and shallow dimples and (d) Dimples of varying size intermingled with noticeable macroscopic voids on the overload surface

composite is compared one-on-one with the unreinforced or monolithic counterpart (AZ31). The key features observed on the tensile fracture surface of the nickel particle-reinforced magnesium alloy based composite are shown in Fig. 4. Overall morphology of the deformed and failed test specimen is as shown in Fig. 4(a). At progressively higher magnifications the transgranular fracture regions were found to be covered with a rich and healthy population of ductile dimples reminiscent of the occurrence of locally ductile failure (Fig. 4b). Upon gradually traversing the tensile fracture surface and immediately prior to the region of tensile overload the fracture surface was covered with shallow dimples intermingled with isolated microscopic voids (Fig. 4c). The region of overload was covered with a noticeable population of dimples (Fig. 4d). The key features observed at the fine microscopic level, namely, microscopic voids and a rich array of dimples of varying size and shape is clearly indicative of the occurrence of ductile failure mechanisms at the fine microscopic level, while global fracture was essentially brittle.

Observation of the tensile fracture surface of magnesium alloy (AZ31) is shown in Fig. 5. Overall fracture was flat and essentially normal to the far-field stress axis and indicative of brittle failure (Fig. 5a). Evident on the fracture surface were macroscopic and fine microscopic voids intermingled with macroscopic cracks. At gradually increasing or higher allowable magnifications of the SEM,

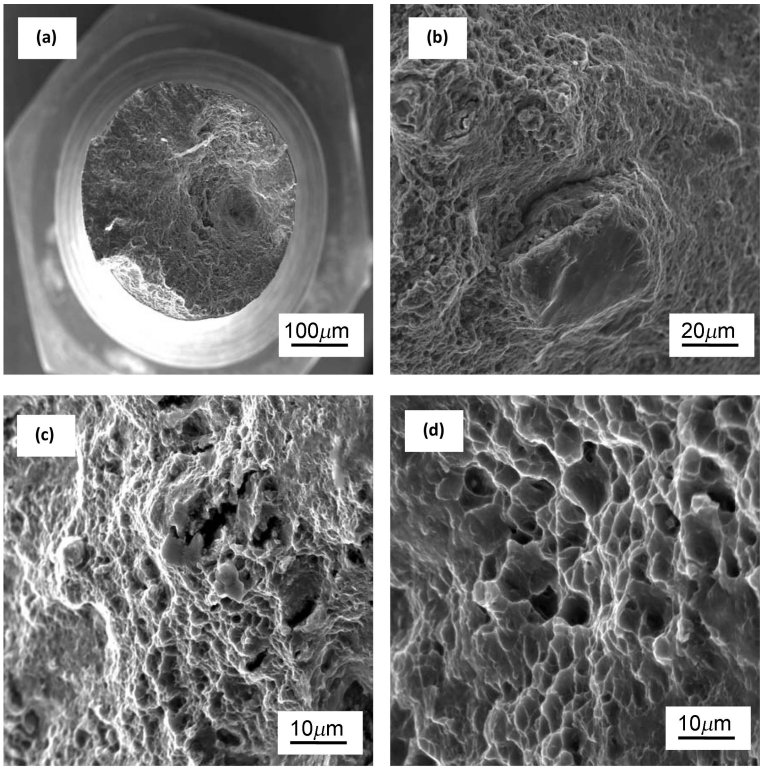

Fig. 5 Scanning electron micrographs of the tensile fracture surface of the magnesium alloy AZ31 showing: (a) Overall morphology of failure normal to far field stress axis, (b) Transgranular region showing fine microscopic crack intermingled with shallow dimples, (c) Voids of varying size and dimples of varying shape in region prior to tensile overload and (d) Dimples and microscopic voids covering the region of tensile overload

the transgranular regions of the fracture surface revealed the array of randomly dispersed fine microscopic cracks to be intermingled with a noticeable population of shallow dimples and voids of varying size (Fig. 5b). These fine microscopic features are reminiscent of the occurrence of both brittle and ductile failure mechanisms at the fine microscopic level. Immediately prior to the region of tensile overload the fracture surface revealed isolated microscopic cracks surrounded by both voids of varying size and dimples of varying shape (Fig. 5c). The region of tensile overload revealed an observable population of dimples, shallow in nature and varying shape, intermingled with fine microscopic voids (Fig. 5d), reminiscent of locally occurring ductile failure mechanisms.

4.5 Microscopic mechanisms governing tensile fracture behavior

Since crack extension under quasi static loading occurs at high stress intensities, comparable to the fracture toughness of the material, the presence of a population of voids, microscopic in nature, dimples and even microscopic cracks degrades the actual strain-to-failure associated with ductile failure. In both the unreinforced and reinforced magnesium alloy (AZ31) although the exact nucleation of the observed fine microscopic voids is difficult to pin-point, their shape and size

suggests that they may have nucleated around the second-phase particles dispersed through the microstructure during the later stages of tensile deformation. Consequently, they are unable to undergo appreciable growth that would result in their ovalization. Nucleation of a fine microscopic void at a second–phase particle such as the reinforcing nickel particles occurs only when the elastic energy of the reinforcing nickel particle exceeds the surface energy of the newly formed void surfaces. While this is a necessary condition, it must also be aided by stress at the matrix-particle interface that exceeds the interfacial strength. When a critical value of the interface stress is reached the nucleation of void is favored to occur. During continued tensile deformation the coalescence of the fine microscopic voids is the last stage in the 'local' ductile failure process. The halves of these fine microscopic voids are the dimples observed on the tensile fracture surface. Growth of the fine microscopic voids is essentially dictated by localized microplastic deformation. The limited growth of the voids coupled with lack of their coalescence, as a dominant fracture mode, suggests the overall brittle nature of the microstructure as it pertains to controlling the deformation characteristics.

During progressive tensile deformation the presence of dislocations and their pile up both at the nickel particles dispersed through the microstructure and the grain boundary regions facilitates in the initiation of fine microscopic cracks along the grain boundaries. These fine microscopic cracks grow and link to form macroscopic cracks. Both the microscopic and macroscopic cracks were observed to be traversing the grain boundaries and extending in the direction of tensile stress axis. This suggests the importance of normal stress at the 'local' level in enhancing tensile deformation (Srivatsan and Lewandowski 2005, Srivatsan *et al.* 2005).

5. Conclusions

Based on an investigation of the intrinsic influence of alumina nanoparticle and nickel microparticle reinforcements on microstructural development, tensile response and tensile fracture behavior of a magnesium alloy (AZ31), following are the key findings:

1. The monolithic alloy (AZ31) and the composite AZ31/1.5 vol.% Al_2O_3/1.5 vol.% Ni were successfully synthesized using the technique of disintegrated melt deposition technique followed by hot extrusion.
2. Microstructure of both the monolithic alloy (AZ31) and the composite consisted of α-Mg and the eutectic phase β-$Mg_{17}Al_{12}$.
3. Microstructure of the micron size nickel particle reinforced magnesium base composite revealed a non-uniform dispersion of both the nickel particles and the Al_2O_3 particles resulting in regions rich in particle-reinforcement and regions depleted of both nickel and Al_2O_3 particle reinforcement.
4. Marginal improvement in yield strength was observed for the composite when compared to the monolithic alloy (AZ31). This observed improvement is ascribed to be due the conjoint and mutually interactive influences of a high modulus of the reinforcing phases $(Al_2O_3)_p$ and nickel powders), and compatibility between the reinforcing phase and the metal matrix resulting in proper load transfer between the constituents of this composite.
5. Addition of nickel particles to the nanoalumina particulate reinforced magnesium alloy (AZ31) metal matrix resulted in an observable 15 pct drop in tensile strength. This is attributed to the presence of fine microscopic cracks at several locations on the fracture surface of the dual particle reinforced magnesium alloy composite when compared to the matrix alloy.

6. The dual particle reinforced magnesium alloy based composite showed hardly any change in elongation to failure but a 45 pct increase in reduction-in-cross-sectional area (*RA* = 23.7 pct) when compared one-on-one with the monolithic counterpart (AZ31) (*RA* = 16.4 pct).
7. Overall fracture of the composite was flat and essentially normal to the far-field stress axis and indicative of brittle failure. Evident on the fracture surface were macroscopic and fine microscopic voids intermingled with macroscopic cracks. The transgranular regions of the fracture surface revealed the array of randomly dispersed fine microscopic cracks to be intermingled with a noticeable population of shallow dimples and voids of varying size. These fine microscopic features are reminiscent of the occurrence of both brittle and ductile failure mechanisms at the fine microscopic level.
8. The key features observed at the fine microscopic level in fracture of the monolithic alloy was microscopic voids and a rich array of dimples of varying size and shape is clearly indicative of the occurrence of ductile failure mechanisms at the fine microscopic level, while global fracture was essentially brittle.

Acknowledgements

Dr. K. Manigandan expresses thanks and appreciation to DCT Inc. (Cleveland, Ohio) and the University of Akron for supporting his efforts in this research study through a graduate assistantship.

References

Chawla, K.K. (1987), *Composite materials: science and engineering*, Springer-Verlag, New York, USA.

Deng, K.K., Wu, K., Wu, Y.W., Nie, K.B. and Zheng, M.Y. (2010), "Effect of submicron size SiC particulates on microstructure and mechanical properties of AZ91 magnesium matrix composites", *J. Alloy. Compd.*, **504**(2), 542-547.

Dieter, G. (2007), *Mechanical metallurgy*, McGraw Hill Publishers, Third Edition.

Fan, X., Tang, W., Zhang, S., Li, D. and Peng, Y. (2010), "Effects of dynamic recrystallization in extruded and compressed AZ31 magnesium alloy", *Acta. Metall. Sin.*, **23**(5), 334-342.

Francis, E.D., Prasad, N.E., Ratnam, C., Kumar, P.S. and Kumar, V.V. (2011), "Synthesis of nano alumina reinforced magnesium-alloy composites", *Int. J. Adv. Sci. Technol.*, **27**, 35-44.

Ganesh, V.V., Gupta, M. and Srivatsan, T.S. (2010), *Journal of recent research developments in materials science and engineering*, ISBN: 81-7895-057-X, 119-136.

Gupta, M. and Srivatsan, T.S. (1999), "Microstructure and grain growth behavior of an aluminum alloy metal matrix composite processed by disintegrated melt deposition", *J. Mater. Eng. Perform.*, **8**(4), 473-478.

Gupta, M., Lai, M.O. and Lim, C. (1997), "Regarding the processing associated microstructure and mechanical properties improvement of an A!-4.5 Cu alloy", *J. Alloy. Compd.*, **260**(1), 250-255.

Habibnejad-Korayem, M., Mahmudi, R. and Poole, W.J. (2009), "Enhanced properties of Mg-based nano-composites reinforced with Al2O3 nano-particles", *Mater. Sci. Eng. A*, **519**(1-2), 198-203.

Hassan, S.F. and Gupta, M. (2006), "Effect of particulate size of Al2O3 reinforcement on microstructure and mechanical behavior of solidification processed elemental Mg", *J. Alloy. Compd.*, **419**(1-2), 84-90.

Ho, K.F., Gupta, M. and Srivatsan, T.S. (2004), "The mechanical behavior of magnesium alloy AZ91 reinforced with fine copper particulates", *Mater. Sci. Eng. A*, **369**(1-2), 302-308

Hong-Liang, Z., Shao-kang, G., Fei-yan, Z., Qing-kui, L. and Li-guo, W. (2005), *Transactions of nonferrous metals society of China*, **15**, 144-148.

Katarzyna N Brasczynska-Malik (2011), *Magnesium alloys - Design, Processing and Properties*, Edited by: Frank Czerwinski, Katarzyna N. Braszczyńska-Malik, Published by InTech, 95-112.
Koss, D.A. and Copley, S.M. (1971), *Metallurgical transactions*, **2A**, 1557-1560.
Ling, P.S., Gupta, M., Lai, M.O. and Srivatsan, T.S. (2000), *Aluminum transactions, Int. J.*, **2**(2), 209-215.
Mao, X.P., Huo, X.D., Sun, X.J. and Chia, Y.Z. (2010), "Strengthening mechanisms of a new 700MPa hot rolled Ti-micro alloyed steel produced by compact strip production", *J. Mater. Process. Tech.*, **210**(12), 1660-1666.
Nguyen, Q.B. and Gupta, M. (2008), "Increasing significantly the failure strain and work of fracture of solidification processed AZ31B using nano-Al2O3 particulates", *J. Alloy. Compd.*, **459**(1-2), 244-250.
Paramsothy, M., Chan, J., Kwok, R. and Gupta, M. (2011a), "The synergistic ability of Al2O3 nanoparticles to enhance mechanical response of hybrid alloy AZ31/AZ91", *J. Alloy. Compd.*, **509**(28), 7572-7578.
Paramsothy, M., Chan, J., Kwok, R. and Gupta, M. (2011b), *Composites Part A: Applied science and manufacturing*, **42**(2), 180-188.
Paramsothy, M., Hasan, S.F., Srikanth, N. and Gupta, M. (2009), "Enhancing tensile/compressive response of magnesium alloy AZ31 by integrating with Al2O3 nanoparticles", *Mater. Sci. Eng. A*, **527**(1-2), 162-168.
Radi, Y. and Mahmudi, R. (2010), "Effect of Al2O3 nano-particles on the microstructural stability of AZ31 Mg alloy after equal channel angular pressing", *Mater. Sci. Eng. A*, **527**(10-11), 2764-2771.
Seshan, S., Jayamathy, M., Kailas, S.V. and Srivatsan, T.S. (2003), "The tensile behavior of two magnesium alloys reinforced with silicon carbide particulates", *Mater. Sci. Eng. A*, **363**(1-2), 345-351.
Srivatsan, T.S. and Lewandowski, J.J. (2005), "Metal matrix composites: Types, reinforcements, processing, properties and applications", *Adv. Struct. Mater*, Taylor & Francis, USA.
Srivatsan, T.S. and Sudarshan, T.S. (1993) *Rapid solidification technology: An engineers guide*, Technomic Publishing Company, Lancaster, 603-720.
Srivatsan, T.S., Meslet, Al-Hajri and Lam, P.C. (2005), "The quasi-static, cyclic fatigue and final fracture behavior of a magnesium alloy metal-matrix composite", *Compos. Part B-Eng.*, **36**(3), 209-222.
Tham, L.M., Gupta, M. and Cheng, L. (1999), "Influence of processing parameters during disintegrated melt deposition processing on near net shape synthesis of aluminum based metal matrix composites", *Mater. Sci. Technol.*, **15**(10), 1139-1146.
Ye, H.Z. and Liu, X.Y. (2004), "Review of recent studies in magnesium matrix composites", *J. Mater. Sci.*, **39**(20), 6153-6171.
Yong, M.S. and Clegg, A.J. (1999), *Foundry man*, **71**.